Title

Reliable quantification of marrow fat content and unsaturation level using in vivo MR spectroscopy

Journal

Magnetic Resonance in Medicine, 79(3)

ISSN

0740-3194

Authors

Xu, Kaipin
Sigurdsson, Sigurdur
Gudnason, Vilmundur
et al.

Publication Date

2018-03-01

DOI

10.1002/mrm.26828

Peer reviewed

HHS Public Access

Author manuscript

Magn Reson Med. Author manuscript; available in PMC 2019 March 01.

Published in final edited form as:

Magn Reson Med. 2018 March ; 79(3): 1722–1729. doi:10.1002/mrm.26828.

Reliable Quantification of Marrow Fat Content and Unsaturation Level Using in Vivo MR Spectroscopy

Kaipin Xu[1], **Sigurdur Sigurdsson**[2], **Vilmundur Gudnason**[2,3], **Trisha Hue**[4], **Ann Schwartz**[4], and **Xiaojuan Li**[1]

[1]Department of Radiology and Biomedical Imaging, University of California, San Francisco (UCSF), San Francisco, California, USA [2]Icelandic Heart Association, Kopavogur, IS 201 Iceland [3]University of Iceland, Reykjavik, Iceland [4]Department of Epidemiology and Biostatistics, UCSF, San Francisco, California, USA

Abstract

Purpose—To develop a novel technique for reliable quantification of bone marrow fat content and composition using in vivo magnetic resonance spectroscopy (MRS).

Methods—A MRS quantification method combining both advantages of Voigt line-shape model and time-domain analysis is developed. The proposed method was tested using computer simulated data and in vivo data acquired at lumbar vertebral bodies of 23 subjects (83.8 ± 3.7 years, 10 females) from L1 to L4. Reliability and reproducibility were calculated for the quantification results. Comparisons between the proposed method and some conventional methods were conducted.

Results—Low mean absolute percentage errors (MAPE) and low mean coefficients of variation (MCV) for computer simulations suggest that the proposed method is accurate and precise. By using this method, marrow fat content can be reliably quantified even for data with low spectral resolution and low signal-to-noise ratio (SNR). Unsaturation level can be reliably quantified for data with moderate spectral resolution and moderate SNR. Results obtained from in vivo data using the proposed method demonstrated better model fit than conventional methods.

Conclusion—The method proposed in this study has better performance than conventional methods in the quantification of bone marrow MRS data, and has great potential for wide applications of studying marrow fat contents and composition.

Keywords

bone marrow; fat quantification; fat unsaturation; Voigt line-shape model; time-domain analysis; computer simulation; in vivo magnetic resonance spectroscopy (MRS)

Correspondence to: Xiaojuan Li, Ph.D., University of California, San Francisco, 185 Berry St., San Francisco, California 94107, USA. xiaojuan.li@ucsf.edu.

INTRODUCTION

Bone marrow fat plays active roles in bone quantity, bone quality, and the hematopoietic system [1,2]. Both magnetic resonance imaging (MRI) and magnetic resonance spectroscopy (MRS) have been used as noninvasive techniques for in vivo study of bone marrow fat [3–6]. Compared to MRI, MRS provides more subtle information which enables quantitative study of fat composition. By quantifying the fat and water components measured using MRS, biomarkers such as fat content (FC, ratio of fat to the sum of water and fat, also called fat fraction) and unsaturation level [UL, ratio of unsaturated (olefinic) lipid to all lipids, also called unsaturation index] can be derived [7,8]. These biomarkers have been applied to better understand marrow fat changes associated with diseases such as osteoporosis [8–13], anorexia nervosa [14,15], diabetes [16,17], heart disease [18], hypertension [19], leukemia [20], obesity [21], and osteoarthritis [22].

In practice, marrow fat quantification for in vivo MRS data is challenging due to line broadening caused by susceptibility differences between bone and marrow, and spectral superposition of peaks. The quantification of fat unsaturation is more difficult with respect to severe overlap of the peaks of olefinic lipid and water. Since the correlations found between fat unsaturation and diseases such as osteoporosis, diabetes, and anorexia nervosa have attracted more attention [8,15,16], it is of great importance and interest to have fat unsaturation level reliably quantified as well as fat content.

In previous studies, several strategies for MRS fat quantification were introduced including integrating the area under water and lipid peaks [7,9,23–25], fitting the spectra in the frequency domain [11,16,17,22], and fitting the free induction decays (FID) in the time domain [8,10,13,26–28]. Peak area integration requires no prior knowledge or assumptions and can be easily done in the frequency domain; however, this strategy cannot separate the olefinic lipid peak from the water peak and only FC can be roughly estimated. Fitting the components in either frequency-domain or time-domain can help to improve the quantification accuracy, and principles of the two kinds of fitting methods are pretty similar. However, most of the frequency-domain methods are limited to fiting the real part of well-phased spectrum since in the frequency domain, an analytical expression of the imaginary part of some line-shape rather than Lorentzian is usually unavailable [29]. Time-domain methods do not have such limitations and line-shape models and phase parameters can be easily incorporated in the model function. An ingenious frequency-domain method (“TDFD fitting”) proposed by Slotboom et al. [31] combines both advantages of frequency- and time-domain methods and is not restricted to absorption line fitting.

Another factor affecting fitting accuracy is line-shape model selection. Obvious residual distortions were observed in previous studies where pure Lorentzian or pure Gaussian models were used [8,13,17], indicating systematic deficiency of the model function used for fitting. Due to imperfect shimming and susceptibility variations, experimental MRS data are better described by Voigt model, which is the convolution of Lorentzian and Gaussian models [30–32]. Unfortunately, Voigt model is not provided in mainstream time-domain quantification methods such as AMARES [33–35]. Recently, a Voigt model based frequency-domain quantification method was proposed to quantify marrow fat in lumbar

vertebrae and knees [11,16,17,22]. The method employs an approximation by fitting a linear combination of normalized Lorentzian and Gaussian functions to the real part of the spectrum [32]. This method improved the quantification reliability to some extent; however, it still suffers from the issues of most frequency-domain methods and their fitting residuals were still distorted.

To overcome major difficulties aforementioned and to reliably quantify bone marrow MRS data, we present here a new method combining both advantages of Voigt line-shape and time-domain analysis. In the method, prior knowledge of chemical shifts of water and lipids are embedded, allowing the method to be fully automated and highly efficient. Appropriate constraints on fitting parameters were included, making the method more robust. The goal of this study was to investigate the reliability and reproducibility of this method using computer simulations and in vivo data of MRS in lumbar vertebrae.

METHODS

Quantification Method

The complex raw data FID point y sampled at time point t can be expressed as:

$$y_m = \sum_{n=1}^{N} a_n \cdot \exp\left[(-d_n + i \cdot 2\pi \cdot f_n) \cdot t_m + i \cdot \Phi_n\right] \quad (1)$$

where i is the imaginary unit, a the amplitude, d the damping, f the resonance frequency, and Φ the phase. Subscripts $m = 1, 2, \ldots, M$ and $n = 1, 2, \ldots, N$ represent the indices of data points and spectral components, respectively. The damping d is directly associated to spectral line-shape and peak width [full width at half maximum (FWHM)]. For pure Lorentzian line-shapes, d is a constant, i.e. $d = d_L$; while for pure Gaussian line-shapes, d is proportional to the sampling time point t, i.e. $d = d_G \cdot t$. The method in this paper fits the FIDs with $d = d_L + d_G \cdot t$ as the Voigt damping [35]. The component parameters a, d, f, and Φ can be solved by iteratively minimizing the distance between observed and fitted data points (χ^2, chi-square) with a nonlinear least-squares routine for d, f, and Φ in the exponential function, and with a linear routine for the amplitude a, alternately [33–35].

Seven (7) peaks including the water peak (W) at 4.7 ppm and 6 lipid peaks (I – VI) emerged at 0.9, 1.3, 2.1, 2.8, 4.2, and 5.3 ppm are quantified (Fig. 1b), referred to the assignment in previous studies [18,19,26] (i.e. the peaks I, IV, V, and VI were assigned to the resonance of lipids at 0.9 ppm [–$(CH_2)_n$–CH_3)], 2.8 ppm [–CH=CH–CH_2–CH=CH–], 4.2 ppm [–CH_2–O–CO–], and the unsaturated lipid at 5.3 ppm [–CH=CH–], respectively. The peak II was assigned to the superposition of the resonance at 1.3 ppm [–$(CH_2)_n$–] and 1.6 ppm [–CO–CH_2–CH_2–], and the peak III was assigned to the superposition of resonance at 2.0 ppm [–CH_2–CH=CH–CH_2–] and 2.3 ppm [–CO–CH_2–CH_2–]). These prior knowledge about peak positions are embedded in our method as starting values for fitting. We found that unconstrained optimization may also achieve good regression, however, sometimes the results could be totally meaningless. To eliminate meaningless solutions, appropriate constraints need to be applied to the component parameters, e.g. nonnegativity constraints on

the amplitude and the damping coefficients, and dual-bound constraints on the peak positions allowing ± 0.1 ppm chemical shift tolerance. The constraints are realized via the logarithmic barrier algorithm [36] in the nonlinear least-squares routine, and via the NNLS algorithm [37] in the linear routine. In the nonlinear least-squares routine, analytical expressions are used to compute the gradients (first-order derivative) and the Hessian (second-order derivative) matrix of 22 parameters including 7 f, 7 d_L, 7 d_G, and 1 Φ with respect to χ^2 and the imposed logarithmic barrier function. Five (5) barrier parameters including 10, 1, 0.1, 0.01, and 0.001 are tested and the solution giving the lowest χ^2 is adopted as the final solution. After processing, the amplitudes of the lipid (a_I, a_{II}, …, a_{VI}) and water peaks (a_W) are quantified. FC and UL are calculated as:

$$FC = \frac{\text{total lipids}}{\text{water+total lipids}} = \frac{a_I + a_{II} + a_{III} + a_{IV} + a_V + a_{VI}}{a_W + a_I + a_{II} + a_{III} + a_{IV} + a_V + a_{VI}} \quad (2)$$

$$UL = \frac{\text{olefinic lipid}}{\text{total lipids}} = \frac{a_{VI}}{a_I + a_{II} + a_{III} + a_{IV} + a_V + a_{VI}} \quad (3)$$

To our knowledge, this is the first time that the true Voigt line-shape model instead of an approximated one is employed to quantify bone marrow MRS data using time-domain quantification. Although time-domain methods can be sensitive to the starting values, the prior knowledge and the constraints applied in our method can reduce the uncertainty and enhance the robustness and reliability of bone marrow fat quantification. All fitting codes were developed using MATLAB (Mathworks, Natick, MA). The computation time for one spectrum is around 5 seconds on a modern PC (CPU: 3.60 GHz × 8; RAM: 15.4 GB). The processing procedure is fully automated and simply requires the input of time-domain data.

Unsaturated Lipid Resolution Grading

One of the major difficulties in the quantification of the unsaturated lipid is its close superposition with the water resonance. In the worst case, the olefinic lipid peak is totally hidden under the wing of the water peak. To investigate the reliability of the new method for MRS data with different levels of peak overlapping, a grading system was developed for evaluating the resolution of unsaturated lipids as Grades 0, 1, and 2, representing well resolved (tip of the olefinic lipid peak is clearly seen), partially resolved (only an olefinic lipid shoulder can be seen), and not resolved (the olefinic lipid resonance is totally invisible), respectively (Fig. 2). Simulation data with the 3 resolution grades were generated to test the reliability of the proposed method, as discussed in detail in the following section. The grading system was then applied to bone marrow MRS data collected in the in vivo study. Two researchers graded the lipid resolution independently.

Computer Simulations

Synthetic data were generated following the time-domain model function of FID (Eq. 1). In each dataset, 7 components (n = 7) were included in the model. Component parameters such

as peak amplitudes, widths, and chemical shifts were randomly picked in a reasonable range mimicking in vivo human bone marrow MRS data [FC ranged from 30% to 90%; UL from 1% to 15%; FWHMs from 0.2 to 0.5 ppm; line-shape from pure Lorentzian ($d_L > 0$; $d_G = 0$) to Voigt ($d_L > 0$; $d_G > 0$) and pure Gaussian ($d_L = 0$; $d_G > 0$); chemical shifts with deviations ranged from −0.05 to 0.05 ppm]. In the beginning, 300 noise free synthetic datasets with 3 unsaturated lipid resolution grades were generated (100 datasets for each grade). After that, Monte Carlo simulation was performed by adding 30 sets of randomly synthesized white Gaussian noise with 3 noise levels [signal-to-noise ratio (SNR) = 500, 200, and 100] to each noise free dataset (10 noise sets for each level), resulting in a total of 9000 synthetic datasets. In this study, SNR is defined as the ratio of the modulus of the largest signal to that of noise in the time domain. The synthetic datasets were quantified using our new method compared to a conventional 2-peak Lorentzian model time-domain fitting, which was commonly used in previous studies [10,13,38,39]. Note that UL cannot be quantified using the conventional method since only 2 peaks (centered at about 1.3 and 4.7 ppm) are fitted to the spectrum.

In Vivo Study

In vivo MRS data were collected using a 1.5-Tesla instrument (GE Healthcare, Milwaukee, Wisconsin) with an 8-channel cervical-thoracic-lumbar spine coil (using the lowest 3 elements; GE Healthcare). Twenty-three subjects (10 females, 83.8 ± 3.7 years) from the Age Gene / Environment Susceptibility (AGES)-Reykjavik cohort study in Iceland were included in the study. The AGES-Reykjavik study design is described in detail elsewhere [40]. Among the 23 subjects, 3 were scan-rescanned on the same day with repositioning in between for evaluating reproducibility. Prior to the acquisition of MRS data, MR imaging with standard clinical sagittal T2-weighted fast spin-echo (FSE) sequence [repetition time (TR) = 5000 ms, echo time (TE) = 87 ms, field of view (FOV) = 22 cm, slice thickness = 6 mm, echo train length = 32] was performed to visually assess the lumbar vertebrae and prescribe the spectral acquisition box (Fig. 1).

After imaging, single-voxel MRS data were acquired at lumbar vertebral bodies from L1 to L4 using the PRESS (point-resolved spectroscopy) sequence (TR = 3000 ms, TE = 35 ms, 64 averages without water suppression, number of data points = 2048, voxel size = 1.2 cm × 1.2 cm × 1.5 cm = 2.16 cm^3, spectral width = 2500 Hz). The PRESS box was positioned in the middle of the vertebral body with a constant box size throughout the study. For all the in vivo MRS data, an average SNR around 500 was achieved. The in vivo data were quantified using the Voigt model quantification. To find out which model is more adaptive to bone marrow MRS data, pure Lorentzian and pure Gaussian models were also tested on 10 randomly picked datasets. Starting values such as resonance frequencies and peak widths were exactly the same for the three models.

Statistical Analyses

Serving as indicators representing the accuracy and reliability of the methods, Percentage errors (PE) and absolute percentage errors (APE) were calculated for simulation data using the quantification results compared to the ground truth, i.e. PE = (quantified FC or UL – true FC or UL)/true FC or UL × 100% and $APE = |PE|$. Coefficients of variation (CV) were

calculated for both simulation and experimental datasets as CV = standard deviation (SD) of quantified FC or UL / mean value of quantified FC or UL × 100%, indicating the reproducibility of the methods. For simulation data, one CV was calculated for every 10 noisy datasets constructed of the same ground truth and the same noise level. For experimental data, CVs were calculated for scan and rescan datasets. Cohen's Kappa-test was performed to measure inter-observer agreement in unsaturated lipid resolution grading. Pearson's r-tests were performed to study the correlation between FCs obtained by the proposed method (7-peak Voigt model) and the conventional method (2-peak Lorentzian model) for simulation data, and the correlations between FC and UL and their correlations with age for in vivo data. Two tailed t-tests were performed to study the differences between FCs and ULs of different vertebral bodies and the differences between male and female subjects. Statistical significance was defined as $P < 0.05$.

RESULTS

Simulation Data

Table 1 displays the mean percentage errors (MPE), mean absolute percentage errors (MAPE), and mean coefficients of variation (MCV) calculated for FC and UL obtained from simulation data, using the developed method and using 2-peak Lorentzian model fitting.

For FC quantified using our new method, low MPEs and MAPEs were observed in all 3 unsaturated lipid resolution grades with all 3 noise levels ($|\ MPE\ | < 3\%$; $MAPE < 5\%$). Low MCVs in 500- and 200-SNR cases (< 2%) and moderate MCVs in 100-SNR cases (< 10%) were observed.

For FC quantified using 2-peak Lorentzian model fitting, MPEs around −10% were observed in all 3 resolution grades with all 3 noise levels. For each MPE, its associated MAPE was exactly its opposite number. The MCVs were very low in 500- and 200-SNR cases (< 0.3%) but increased significantly in 100-SNR cases (> 13%).

The fat contents obtained by the proposed method (7-peak Voigt model, FC) were significantly correlated to the conventional method (2-peak Lorentzian model, FC*) ($R = 0.979$, $P < 10^{-9}$). The linear relation was: FC* (%) = 0.983 × FC (%)− 5.285, as shown in Fig. 3.

For UL, low MPEs and moderate MAPEs were observed in simulation data graded as 0 and 1 with 500- and 200-SNR noise levels ($|\ MPE\ | < 3\%$; $MAPE < 13\%$). The MAPEs were high in Grade 2 and 100-SNR cases (> 17%). The MCVs were low in 500-SNR cases (< 4%), moderate in 200-SNR cases (< 11%), and high in 100-SNR cases (> 30%), regardless of the unsaturation lipid resolution grade.

In Vivo Data

Among the 92 in vivo datasets collected from 23 subjects, 18 spectra were assessed as unsaturation lipid resolution Grade 0 (well resolved), 65 as Grade 1 (partially resolved), and 9 as Grade 2 (not resolved). A Kappa-value of 0.88 was observed for the grading results, indicating very good inter-observer agreement. Based on the simulation results, marrow fat

quantification was performed on 83 datasets with Grade 2 spectra removed from the database.

For the 10 datasets that were randomly picked, the fitting root-mean-square errors (RMSE) obtained by Voigt model were lower than those obtained by pure Lorentzian or pure Gaussian model (Table 2). Fig. 4 shows the fitting results of a MR spectrum collected from the L2 vertebral body of a 95-year-old female subject using the three models. Compared to pure Lorentzian and pure Gaussian models, the overall fitting RMSE obtained by Voigt model was reduced by 33.8% and 32.3%, respectively.

For the 83 datasets, the FCs were 60.9% ± 7.5%, ranging from 45.1% to 77.6% while the ULs were 3.8% ± 1.3%, ranging from 1.7% to 10.3% (Table 3). Low CVs of FC (1.5% ± 1.5%) and UL (5.1% ± 3.6%) were observed in the 3 subjects who were rescanned.

FCs of different vertebral bodies were significantly correlated to each other (Table 4) and an increasing trend of marrow FC from L1 to L4 was observed (Table 3). No significant correlation or significant difference was found between ULs of different vertebral bodies. Significantly higher average FCs ($P < 0.05$) and lower average ULs ($P < 0.05$) were found in female subjects compared to male subjects (Table 3). In this study, no correlation was found between age and FC or between age and UL.

DISCUSSION

In this study, we developed a novel quantification method for the analysis of marrow fat composition using in vivo MR spectroscopy. Results obtained from both simulation and in vivo human data showed good reliability and reproducibility of the proposed method, as well as its significant advantages over conventional methods. In particular, this method allows reliable quantification of unsaturated lipids even at 1.5T, a difficult challenge with previous methods.

Computer simulations demonstrate that the FCs quantified using our proposed method are very reliable in general (Table 1). The PEs and APEs were low for all unsaturated lipid resolution grades and noise levels. The CVs were very low in 500- and 200-SNR cases, however, less optimal when SNR = 100 though still under 10%.

In comparison, the conventional method (2-peak Lorentzian model) has excellent reproducibility for data with high or moderate SNR. However, for 100-SNR datasets the CVs were much higher than those obtained by the new method, indicating the conventional method is less robust and more sensitive to noise perturbation. Furthermore, it should be noted that the conventional method is systematically biased. It consistently underestimates FC as inferred by the fact that the MPEs were always negative and exactly the additive inverse of their associated MAPEs. This is mainly caused by the ignorance of the glycerol and the olefinic lipid peaks during quantification, which leads to the overestimation of water content.

The significant correlation (Fig. 3) between the FCs obtained by our method and the conventional 2-peak method suggests that applying both methods to a clinical or research

study based on marrow fat quantification may yield comparable results in the connection between fat content and disease, despite the inaccuracy of the conventional method.

The PEs, APEs, and CVs of UL demonstrate that our method is reliable and reproducible without obvious systematic bias when quantifying UL for well- and partially-resolved spectra with good or moderate data SNR. However, these statistical indicators were much higher than those for FC quantification, suggesting that it is more challenging to quantify fat composition than overall fat contents in vivo. According to the definitions of FC and UL (Eqs. 2 and 3), the quantification accuracy is majorly attributed to the accuracy of the amplitudes of water and its neighboring lipids (glycerol and olefinic). Identification of the two peaks at their overlapping part is vulnerable to data quality especially in low SNR cases where the noise and the signals rising from the olefinic lipid may have approximate amplitudes. Since in bone marrow MRS the concentration of water is usually much higher than that of the olefinic lipid, the identification error at the overlapping part is expected to cause more deviation for UL than for FC.

The overall simulation results in Table 1 illustrate a trend that basically PE, APE, and CV increase as unsaturated lipid resolution grade increases or data SNR decreases. The trend indicates that reliably quantifying the marrow fat can be difficult when spectral resolution is low and/or data SNR is poor. CV seems to be more susceptible to noise when compared to PE and APE, raising the requirement of ensuring data SNR for good precision and reproducibility.

For in vivo bone marrow MRS data, no apparent indicators representing quantification accuracy such as PE or APE can be derived because the ground truth of component amplitudes is not known a priori. Significantly lower RMSEs obtained by our method using Voigt model compared to Lorentzian and Gaussian models agreed well with the results of previous studies that applied Voigt model in the frequency domain [30,41]. Besides, as illustrated in Fig. 4, the fitting residuals obtained by Voigt model distributed randomly while obvious residual distortions were observed in Lorentzian and Gaussian models. It can be expected that more parameters included in the fitting procedure will lead to better fits at the expense of larger uncertainty of the parameters. However, the Voigt model widely observed in NMR/MRS has been well studied for decades and the physical ground that Gaussian broadening caused by the imperfection of data acquisition system affects ideal Lorentzian lines stands firmly. Moreover, Voigt model is self-adaptive to pure Lorentzian ($d_L > 0$ while $d_G = 0$) and pure Gaussian ($d_L = 0$ while $d_G > 0$) models. This comparison indicates that Voigt line-shape is more realistic for in vivo bone marrow MR spectra and it reduces the systematic errors of Lorentzian and Gaussian models. Note that supposing the Voigt model results are correct, Lorentzian model fitting underestimates FC and UL while Gaussian model fitting overestimates them (Table 2).

Based on the unsaturated lipid resolution grading system we proposed, 90.2% of the in vivo spectra were well- (Grade 0) or partially-resolved (Grade 1). Only 9.8% were assessed as not resolved (Grade 2) and were excluded from quantifying the marrow composition. Furthermore the data were collected at 1.5-Tesla while better spectral resolution and lower percentage of data exclusion are expected at a high field strength such as 3-Tesla, which is

widely available for clinical and research studies world-wide. This implies the proposed method can be potentially applied in larger scale clinical studies, without a need of excluding a significant amount of data.

With those spectra assessed as Grade 2 (unsaturated lipid not resolved) excluded, the situations of remaining in vivo datasets were within the range (SNR ≥ 200, Grade ≤ 1) that FC and UL can be reliably quantified using our method referred to the simulation results. The CVs calculated for scan and rescan data were lower than those reported in a previous study [11] where a frequency-domain method was employed (CVs of FC: 1.5% vs. 1.7%; CVs of UL: 5.1% vs. 10.7%), indicating better in vivo precision and reproducibility of the proposed method especially for the quantification of UL.

For our in vivo data, an increasing trend of FC was observed from L1 to L4, which was first reported by Liney et al. [9] and confirmed in subsequent studies [11,17]. This may reflect the “peripheral to axial” conversion from red to yellow marrow with increasing age, or be explained by increasing loading experienced from superior (L1) to inferior (L4). Interestingly, no such trend was observed for UL. This result suggests that marrow fat distribution is more susceptible to the loading variation among different vertebral bodies while fat composition stays relatively consistent or may be affected by other factors. This may also suggest in large-scale study, if one vertebral body level data for UL was excluded due to poor data quality, it will not systematically affect the average values of the remaining vertebral bodies.

The result that FCs of different vertebral bodies significantly correlated to each other (Table 4) was consistent with the findings reported by Li et al. [11,17], while interestingly again, no such correlation were found in UL among different levels of vertebral bodies.

Significantly higher FCs observed in female subjects agreed well with the finding that contrary to young subjects, females older than 60 years have higher marrow fat contents than males [10]. In accordance with the inverse relationship between UL and FC reported by Yeung et al. [8], we also observed lower ULs in female subjects compared to male subjects. In this study, we did not find a significant correlation between FC and age as reported in previous studies [9,10,23]. This is probably because of the rather narrow age range of our subjects (79–95 years).

Despite the promising results, there are some limitations of the study such as the lack of gold standard for in vivo data and the small size of scan-rescan data for the investigation of in vivo reproducibility. Meanwhile, the acquisition parameters for in vivo study can be further optimized, e.g. by reducing the number of repetitions to save scan time based on the result that fat content and composition can be reliably quantified for bone marrow MRS data with SNR ≥ 200 using the proposed method. In this study, we focused on the effect of data processing (model selection) rather than data acquisition (e.g. PRESS vs. STEAM, chemical shift displacement) on the quantification results. Single TE was used for MRS data acquisition and data correction for T2 [27,42] was not available.

CONCLUSIONS

In this paper, a Voigt model based time-domain quantification method particularly developed for the analysis of bone marrow MRS data is introduced. Computer simulation verified excellent reliability and reproducibility for the quantification of marrow fat content (FC) and unsaturation level (UL) even for spectra with partially resolved unsaturated lipids. Results from in vivo data confirmed reproducibility of the method and improved model fit compared with conventional methods. Significant superiority of the proposed method suggests its potential of wide application.

Acknowledgments

Grant sponsor: NIH/NIAMS; Grant number: R01AR057819.

The AGES-Reykjavik has been funded by NIH contract N01-AG012100, the NIA Intramural Research Program, an Intramural Research Program Award (ZIAEY000401) from the National Eye Institute, an award from the National Institute on Deafness and Other Communication Disorders (NIDCD) Division of Scientific Programs (IAA Y2-DC_1004-02), Hjartavernd (the Icelandic Heart Association), and the Althingi (the Icelandic Parliament). The study is approved by the Icelandic National Bioethics Committee, VSN: 00-063. The AGES-BMA ancillary study is sponsored by the National Institute of Arthritis and Musculoskeletal and Skin Diseases (NIAMS), National Institutes of Health (NIH/NIAMS R01AR057819). The researchers are indebted to the participants for their willingness to participate in the study.

References

1. Rosen CJ, Ackert-Bicknell C, Rodriguez JP, Pino AM. Marrow fat and the bone microenvironment: developmental, functional, and pathological implications. Crit Rev Eukaryot Gene Expr. 2009; 19:109–124. [PubMed: 19392647]
2. Trubowitz, S., Davis, S. The human bone marrow: anatomy, physiology, and pathophysiology. Boca Raton, Fla: CRC; 1982. The bone marrow matrix; p. 43-75.
3. Vogler JB 3rd, Murphy WA. Bone marrow imaging, Radiology. 1988; 168:679–693. [PubMed: 3043546]
4. Schick F, Einsele H, Bongers H, et al. Leukemic red bone marrow changes assessed by magnetic resonance imaging and localized ^{1}H spectroscopy. Ann Hematol. 1993; 66:3–12. [PubMed: 8381677]
5. Jensen KE, Jensen M, Grundtvig P, Thomsen C, Karle H, Henriksen O. Localized in vivo spectroscopy of the bone marrow in patients with leukemia. Magn Reson Imaging. 1990; 8:779–789. [PubMed: 2266805]
6. Schellinger D, Lin CS, Hatipoglu HG, Fertikh D. Potential value of vertebral proton MR spectroscopy in determining bone weakness. AJNR Am J Neuroradiol. 2001; 22:1620–1627. [PubMed: 11559519]
7. De Bisschop E, Luypaert R, Louis O, Osteaux M. Fat fraction of lumbar bone marrow using in vivo proton nuclear magnetic resonance spectroscopy. Bone. 1993; 14:133–136. [PubMed: 8334030]
8. Yeung DK, Griffith JF, Antonio GE, Lee FK, Woo J, Leung PC. Osteoporosis is associated with increased marrow fat content and decreased marrow fat unsaturation: a proton MR spectroscopy study. J Magn Reson Imaging. 2005; 22(2):279–285. [PubMed: 16028245]
9. Liney GP, Bernard CP, Manton DJ, Turnbull LW, Langton CM. Age, gender, and skeletal variation in bone marrow composition: a preliminary study at 3. 0 Tesla. J Magn Reson Imaging. 2007; 26:787–793. [PubMed: 17729356]
10. Griffith JF, Yeung DKW, Ma HT, Leung JCS, Kwok TCY, Leung PC. Bone marrow fat content in the elderly: a reversal of sex difference seen in younger subjects. J Magn Reson Imaging. 2012; 36:225–230. [PubMed: 22337076]

11. Li X, Kuo D, Schafer AL, Porzig A, Link TM, Black D, Schwartz AV. Quantification of vertebral bone marrow fat content using 3 Tesla MR spectroscopy: reproducibility, vertebral variation, and applications in osteoporosis. J Magn Reson Imaging. 2011; 33:974–979. [PubMed: 21448966]
12. Wiercinska-Drapalo A, Jaroszewicz J, Tarasow E, Siergiejczyk L, Prokopowicz D. The possible association between serum cholesterol concentration and decreased bone mineral density as well as intravertebral marrow fat in HIV-1 infected patients. Infection. 2007; 35:46–48. [PubMed: 17297592]
13. Griffith JF, Yeung DKW, Antonio GE, Lee FKH, Hong AWL, Wong SYS, Lau EMC, Leung PC. Vertebral bone mineral density, marrow perfusion, and fat content in healthy men and men with osteoporosis: dynamic contrast-enhanced MR imaging and MR spectroscopy. Radiology. 2005; 236:945–951. [PubMed: 16055699]
14. Bredella MA, Fazeli PK, Miller KK, Misra M, Torriani M, Thomas BJ, Ghomi RH, Rosen CJ, Klibanski A. Increased bone marrow fat in anorexia nervosa. J Clin Endocrinol Metab. 2009; 94(6):2129–2136. [PubMed: 19318450]
15. Bredella MA, Fazeli PK, Daley SM, Miller KK, Rosen CJ, Klibanski A, Torriani M. Marrow fat composition in anorexia nervosa. Bone. 2014; 66:199–204. [PubMed: 24953711]
16. Patsch JM, Li X, Baum T, Yap SP, Karampinos DC, Schwartz AV, Link TM. Bone marrow fat composition as a novel imaging biomarker in postmenopausal women with prevalent fragility fractures. J Bone Miner Res. 2013; 28(8):1721–1728. http://www.medsci.cn/sci/submit.do?id=cfe93518. [PubMed: 23558967]
17. Baum T, Yap SP, Karampinos DC, Nardo L, Kuo D, Burghardt AJ, Masharani UB, Schwartz AV, Li X, Link TM. Does vertebral bone marrow fat content correlate with abdominal adipose tissue, lumbar spine bone mineral density, and blood biomarkers in women with type 2 diabetes mellitus? J Magn Reson Imaging. 2012; 35:117–124. [PubMed: 22190287]
18. Noula C, Bonzom P, Brown A, Gibbons WA, Martin J, Nicolaou A. ^{1}H-NMR lipid profiles of human blood platelets; links with coronary artery disease. Biochim Biophys Acta. 2000; 1487:15–23. [PubMed: 11004608]
19. Chi Y, Gupta RK. Alterations in membrane fatty acid unsaturation and chain length in hypertension as observed by ^{1}H NMR spectroscopy. Am J Hypertens. 1998; 11:340–348. [PubMed: 9544875]
20. Bongers H, Schick F, Skalej M, Jung WI, Einsele H. Localized in vivo ^{1}H spectroscopy and chemical shift imaging of the bone marrow in leukemic patients. Eur Radiot. 1992; 2:350–356.
21. Bredella MA, Torriani M, Ghomi RH, Thomas BJ, Brick DJ, Gerweck AV, Rosen CJ, Klibanski A, Miller KK. Vertebral bone marrow fat is positively associated with visceral vat and inversely associated with IGF-1 in obese women. Obesity. 2011; 19:49–53. [PubMed: 20467419]
22. Tufts LS, Shet K, Liang F, Majumdar S, Li X. Quantification of bone marrow water and lipid composition in anterior cruciate ligament-injured and osteoarthritic knees using three-dimensional magnetic resonance spectroscopic imaging. Magn Reson Imaging. 2016; 34:632–637. [PubMed: 26723848]
23. Kugel H, Jung C, Schulte O, Heindel W. Age- and sex-specific differences in the ^{1}H-spectrum of vertebral bone marrow. J Magn Reson Imaging. 2001; 13:263–268. [PubMed: 11169833]
24. Bernard CP, Liney GP, Manton DJ, Turnbull LW, Langton CM. Comparison of fat quantification methods: a phantom study at 3. 0T. J Magn Reson Imaging. 2008; 27:192–197. [PubMed: 18064714]
25. Hu HH, Kim HW, Nayak KS, Goran MI. Comparison of fat-water MRI and single-voxel MRS in the assessment of hepatic and pancreatic fat fractions in humans. Obesity. 2010; 18:841–847. [PubMed: 19834463]
26. Karampinos DC, Melkus G, Baum T, Bauer JS, Rummeny EJ, Krug R. Bone marrow fat quantification in the presence of trabecular bone: initial comparison between water-fat imaging and single-voxel MRS. Magn Reson Med. 2014; 71:1158–1165. [PubMed: 23657998]
27. Hamilton G, Middleton MS, Bydder M, Yokoo T, Schwimmer JB, Kono Y, Patton HM, Lavine JE, Sirlin CB. Effect of PRESS and STEAM sequences on magnetic resonance spectroscopic liver fat quantification. J Magn Reson Imaging. 2009; 30:145–152. [PubMed: 19557733]

28. Hamilton G, Yokoo T, Bydder M, Cruite I, Schroeder ME, Sirlin CB, Middleton MS. In vivo characterization of the liver fat ^{1}H MR spectrum. NMR Biomed. 2011; 24:784–790. [PubMed: 21834002]
29. Mierisova S, Ala-Korpela M. MR spectroscopy quantitation: a review of frequency domain methods. NMR Biomed. 2001; 14:247–259. [PubMed: 11410942]
30. Marshall I, Higinbotham J, Bruce S, Freise A. Use of Voigt lineshape for quantification of in vivo ^{1}H spectra. Magn Reson Med. 1997; 37:651–657. [PubMed: 9126938]
31. Slotboom J, Boesch C, Kreis R. Versatile frequency domain fitting using time domain models and prior knowledge. Magn Reson Med. 1998; 39:899–911. [PubMed: 9621913]
32. Bruce SD, Higinbotham J, Marshall I, Beswick PH. An analytical derivation of a popular approxiamation of the Voigt function for quantification of NMR spectra. J Magn Reson. 2000; 142:57–63. [PubMed: 10617435]
33. Vanhamme L, van den Boogaart A, Van Huffel S. Improved method for accurate and efficient quantification of MRS data with use of prior knowledge. J Magn Reson. 1997; 129:35–43. [PubMed: 9405214]
34. Vanhamme L, Van Huffel S, Van Hecke P, van Ormondt D. Time-domain quantification of series of biomedical magnetic resonance spectroscopy signals. J Magn Reson. 1999; 140:120–130. [PubMed: 10479554]
35. Vanhamme L, Sundin T, Van Hecke P, Van Huffel S. MR spectroscopy quantitation: a review of time-domain methods. NMR Biomed. 2001; 14:233–246. [PubMed: 11410941]
36. Nocedal, J., Wright, S. Numerical Optimization. New York, NY: Springer; 1999.
37. Lawson, CL., Hanson, RJ. Solving Least Squares Problems. Prentice-Hall: Englewood Cliffs; 1974.
38. Schwartz AV, Sigurdsson S, Hue TF, et al. Vertebral bone marrow fat associated with lower trabecular BMD and prevalent vertebral fracture in older adults. J Clin Endocrinol Metab. 2013; 98(6):2294–2300. [PubMed: 23553860]
39. Ma YHV, Schwartz AV, Sigurdsson S, et al. Circulating sclerostin associated with vertebral bone marrow fat in older men but not women. J Clin Endocrinol Metab. 2014; 99(12):E2584–E2590. [PubMed: 25144629]
40. Harris TB, Launer LJ, Eiriksdottir G, et al. Age, Gene/Environment Susceptibility-Reykjavik Study: multidisciplinary applied phenomics. AM J Epidemiol. 2007; 165:1076–1087. [PubMed: 17351290]
41. Li, X., Nelson, S. Reliable in vivo lactate and lipid estimation in glioma patients. Proceedings of the 25th Annual International Conference of the IEEE EMBS; Cancun, Mexico. 2003;September 17–21;
42. Dieckmeyer M, Ruschke S, Cordes C, et al. The need for T_2 correction on MRS-based vertebral bone marrow fat quantification: implications for bone marrow fat fraction age dependence. NMR Biomed. 2015; 28:432–439. [PubMed: 25683154]

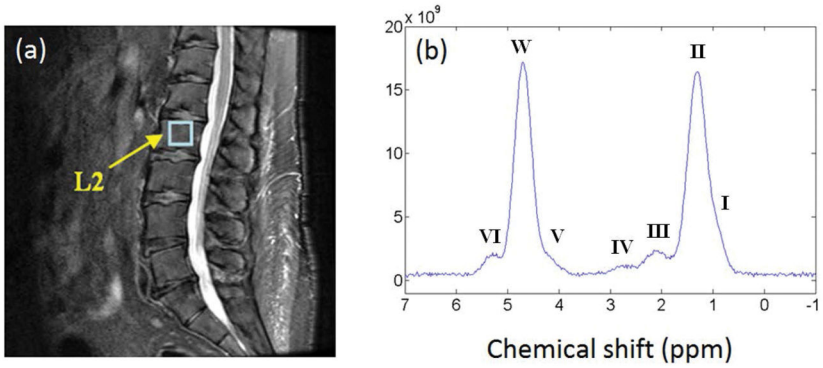

Figure 1.

Bone marrow MRS data acquisition and the converted ^{1}H spectrum. (a) Single voxel MRS data were acquired at lumbar vertebral bodies from L1 to L4 using the PRESS (point-resolved spectroscopy) sequence. (b) The raw data (FID) were then converted to a MR spectrum showing the water peak (W) at 4.7 ppm and 6 lipid peaks (I – VI) emerged at 0.9, 1.3, 2.1, 2.8, 4.2, and 5.3 ppm. The peaks I, IV, V, and VI were assigned to the resonance of lipids at 0.9 ppm [$–(CH_2)_n–CH_3$)], 2.8 ppm [$–CH=CH–CH_2–CH=CH–$], 4.2 ppm [$–CH_2–O–CO–$], and the unsaturated lipid at 5.3 ppm [–CH=CH–], respectively. The peak II was assigned to the superposition of the resonance at 1.3 ppm [$–(CH_2)_n–$] and 1.6 ppm [$–CO–CH_2–CH_2–$], and the peak III was assigned to the superposition of resonance at 2.0 ppm [$–CH_2–CH=CH–CH_2–$] and 2.3 ppm [$–CO–CH_2–CH_2–$].

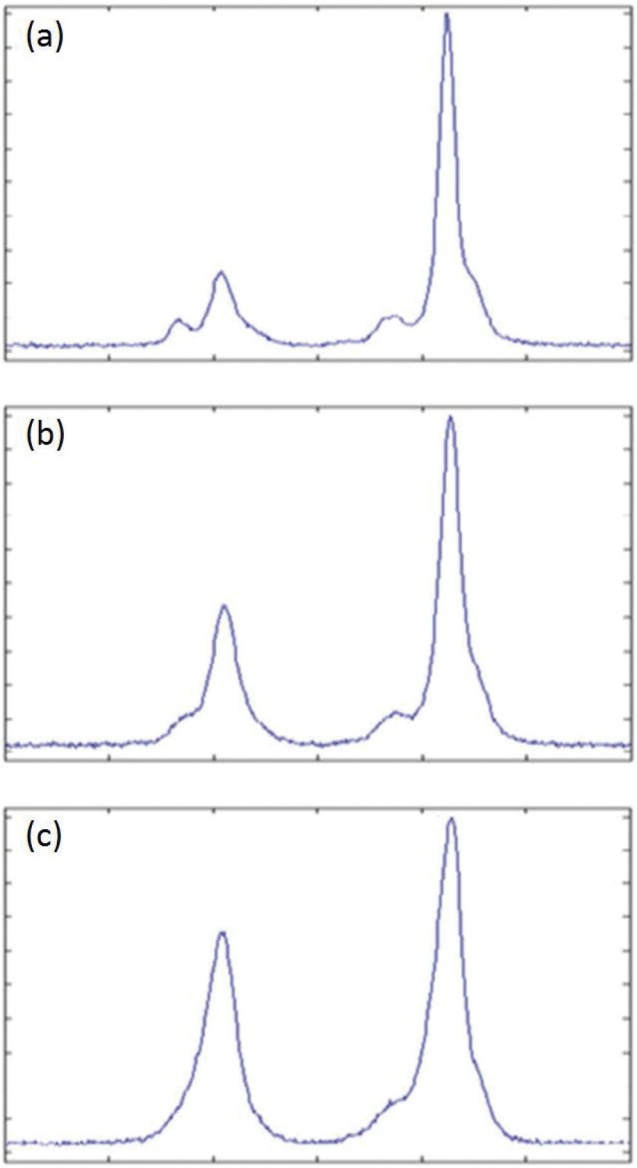

Figure 2.

Examples of bone marrow MRS spectra with different unsaturated lipid resolution grades. (a), (b), and (c) represent well resolved (Grade 0), partially resolved (Grade 1), and not resolved (Grade 2) spectra, respectively.

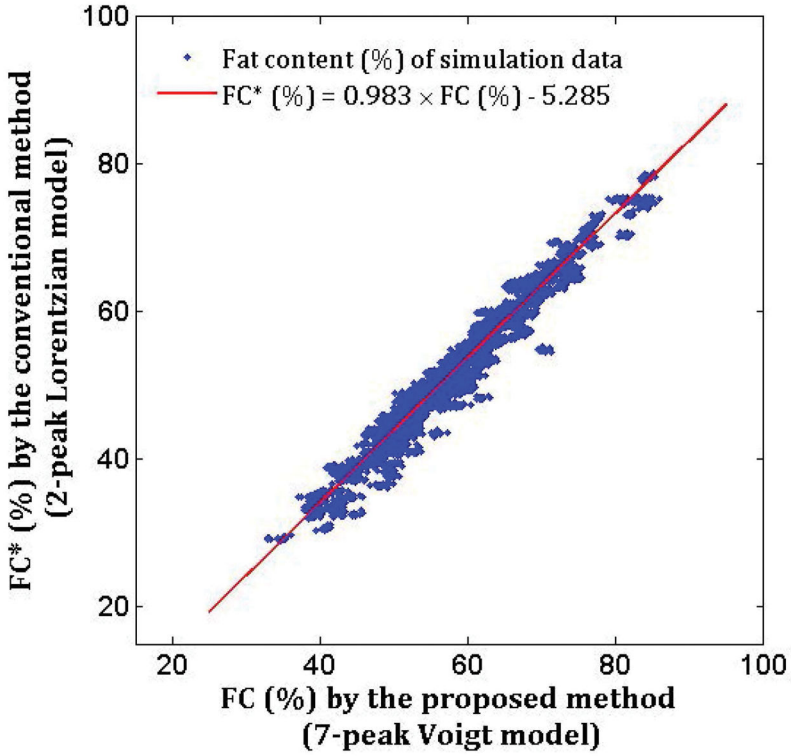

Figure 3.

Fat content results of the simulation datasets. Significant correlation ($R = 0.979$, $P < 10^{-9}$) was found between the fat contents obtained by the proposed method (7-peak Voigt model, FC) and the conventional method (2-peak Lorentzian model, FC*). The linear relation was: FC* (%) = 0.983 × FC (%) – 5.285.

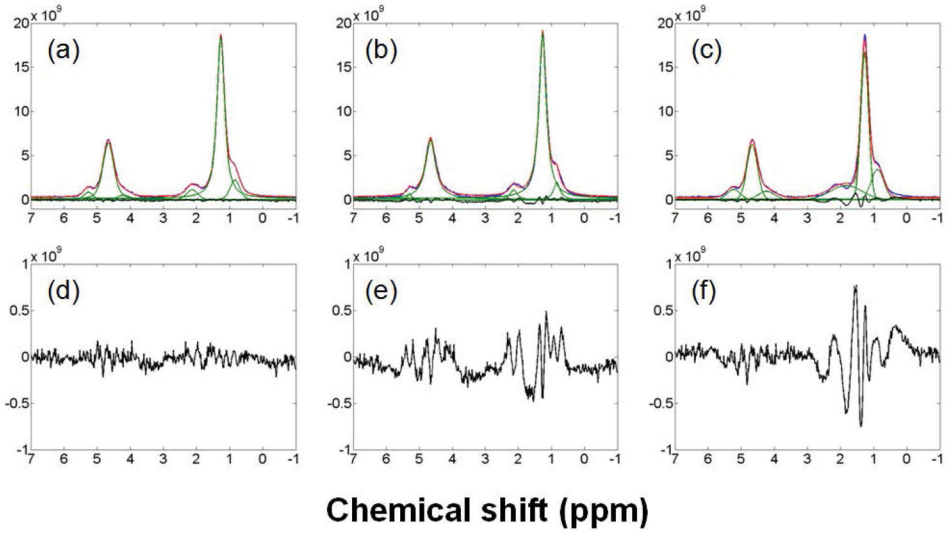

Figure 4.

Real bone marrow MRS data (L2, 95 year, female) quantified by (a) Voigt (FC = 75.0%; UL = 3.7%; RMSE = 1.043×10^6), (b) pure Lorentzian (FC = 70.2%; UL = 1.9%; RMSE = 1.790×10^6), and (c) pure Gaussian (FC = 79.3%; UL = 6.2%; RMSE = 2.022×10^6) line-shape models. Blue, red, and green curves represent the experimental spectrum, the fitted spectrum, and the spectra of separated components, respectively. Fitting residuals are plotted in black and enlarged in (d), (e), and (f).

Table 1

Mean percentage errors (MPE), mean absolute percentage errors (MAPE), and mean coefficients of variation (MCV) of fat contents (FC) and unsaturation levels (UL) quantified for synthetic bone marrow MRS data.

		SNR = 500			SNR = 200			SNR = 100		
		FC	FC*	UL	FC	FC*	UL	FC	FC*	UL
Grade 0	MPE (%)	−0.01	−9.23	1.89	−0.11	−9.49	2.09	−0.22	−9.61	9.64
	MAPE (%)	1.02	9.23	5.84	1.30	9.49	7.56	1.49	9.61	18.86
	MCV (%)	0.33	0.08	2.27	0.90	0.22	7.23	6.12	13.21	30.13
Grade 1	MPE (%)	−0.47	−10.44	−2.41	−0.61	−10.82	−2.62	−0.79	−11.03	4.56
	MAPE (%)	1.91	10.44	10.17	2.10	10.82	12.71	2.49	11.03	23.96
	MCV (%)	0.30	0.09	2.85	0.83	0.23	8.16	7.28	16.53	43.99
Grade 2	MPE (%)	1.92	−10.89	9.56	2.07	−11.46	11.48	1.61	−11.65	30.16
	MAPE (%)	2.58	10.89	17.39	3.10	11.46	21.81	4.34	11.65	43.80
	MCV (%)	0.42	0.09	3.30	1.23	0.25	10.12	9.89	22.68	43.69

*Obtained by 2-peak Lorentzian model quantification.

Table 2

Mean and standard deviation (SD) values of fat content (FC), unsaturation level (UL), and root-mean-square error (RMSE) obtained for 10 randomly picked experimental bone marrow MRS datasets using Voigt, Lorentzian, and Gaussian model quantifications.

	Voigt	Lorentzian	Gaussian
FC (%)	65.1 ± 9.6	61.1 ± 9.4	72.7 ± 6.9
UL (%)	4.4 ± 0.5	1.7 ± 0.9	9.8 ± 2.9
RMSE	$1.066 \times 10^6 \pm 5.787 \times 10^4$	$1.609 \times 10^6 \pm 1.772 \times 10^5$	$1.574 \times 10^6 \pm 3.978 \times 10^5$

Table 3

Mean and SD values of fat content (FC) and unsaturation level (UL) quantified for in vivo bone marrow MRS data using the proposed method. Female subjects have significantly higher average FCs ($P < 0.05$) and lower average ULs ($P < 0.05$) compared to male subjects.

	Male & Female		Male		Female	
	FC (%)	**UL (%)**	**FC (%)**	**UL (%)**	**FC (%)**	**UL (%)**
L1	57.6 ± 8.5	3.6 ± 1.2	53.5 ± 6.6	4.0 ± 1.2	62.8 ± 8.0	3.1 ± 1.0
L2	59.9 ± 6.3	4.2 ± 1.9	57.0 ± 4.7	4.7 ± 2.2	63.7 ± 6.3	3.4 ± 1.1
L3	60.7 ± 5.9	3.9 ± 1.0	58.3 ± 2.6	4.1 ± 0.9	63.8 ± 7.8	3.6 ± 1.0
L4	65.6 ± 7.3	3.8 ± 1.2	63.3 ± 7.2	4.1 ± 1.5	68.6 ± 6.6	3.3 ± 0.5
Average *	60.9 ± 6.2	3.8 ± 0.7	58.0 ± 4.2	4.2 ± 0.4	64.7 ± 6.6	3.3 ± 0.8

* Averaged from L1 to L4.

Table 4

Pearson correlation coefficients of marrow fat content (FC) between vertebral bodies.

	L2	L3	L4
L1	0.910 ***	0.565 *	0.672 **
L2		0.689 **	0.746 **
L3			0.660 *

* P < 0.05;

** P < 0.005;

*** P < 0.0005.